Applied Surface Science 442 (2018) 787–796

Contents lists available at ScienceDirect

Applied Surface Science

journal homepage: www.elsevier.com/locate/apsusc

Full Length Article

Pd-NiO decorated multiwalled carbon nanotubes supported on reduced graphene oxide as an efficient electrocatalyst for ethanol oxidation in alkaline medium

Dhanushkotti Rajesh [a], Pulidindi Indra Neel [b], Arumugam Pandurangan [c], Chinnathambi Mahendiran [a,*]

[a] Department of Chemistry, University College of Engineering, Anna University, Konam, Nagercoil 629 004, Tamil Nadu, India
[b] Department of Materials Science and Chemical Engineering, Hanyang University, Sangnok-gu, Ansan, Gyeonggi-Do 15588, Republic of Korea
[c] Department of Chemistry, Anna University, Guindy, Chennai 600 025, Tamil Nadu, India

ARTICLE INFO

Article history:
Received 15 November 2017
Revised 5 February 2018
Accepted 17 February 2018
Available online 21 February 2018

Keywords:
Ethanol electro oxidation
Pd-NiO functionalized MWCNTs
Reduced GO support
CVD method

ABSTRACT

The synthesis of Pd-NiO nanoparticles decorated multiwalled carbon nanotubes (MWCNTs) on reduced graphene oxide (rGO) for ethanol electrooxidation is reported. NiO nanoparticles (NPs) were deposited on functionalized MWCNTs by wet impregnation method. Pd nanoparticles were formed on NiO-MWCNTs by the addition of $PdCl_2$ and its reduction using $NaBH_4$. The Pd-NiO/MWCNTs nanocomposite then deposited on rGO support using ultrasound irradiation which led to the formation of the Pd-NiO/MWCNTs/rGO electrocatalyst. The prepared electrocatalysts were characterized by XRD, SEM, HR-TEM and XPS analysis. Electrochemical measurements demonstrate that as synthesized Pd-NiO/MWCNTs/rGO electrocatalyst exhibit higher catalytic activity (90.89 mA/cm^2) than either Pd/MWCNTs/rGO (43.05 mA/cm^2) or Pd/C (28.0 mA/cm^2) commercial catalyst. Chronoamperometry study of Pd-NiO/MWCNTs/rGO electrocatalyst showed long-term electrochemical stability. The enhanced catalytic activity of Pd-NiO/MWCNTs/rGO electrocatalyst for electrooxidation of ethanol can be attributed to the synergistic effect between Pd & NiO active sites.

1. Introduction

Liquid hydrocarbons are a promising energy source for a variety of portable and stationary applications [1,2]. Ethanol is a potential liquid fuel used in the operation of direct ethanol fuel cells (DEFC), a clean alternative energy conversion device. Currently, there has been increased interest on fuel ethanol as the same could be produced from ligno-cellulosic biomass, an abundant source of carbohydrate on earth's surface [3–5]. Ethanol is a nontoxic substance with ease of handling and transportation [6]. Moreover, ethanol driven fuel cells operate with high thermodynamic efficiency and high volumetric energy density (8.0 kW h/kg) when compared with methanol based fuel cells (6.1 kW h/kg) [7]. In the development of DEFCs, complete oxidation of ethanol molecule is essential for effective and stable anode electro catalyst performance.

Traditionally, Pt-based noble metals are used as anode catalysts for promoting ethanol electrooxidation in DEFCs [8–11]. However, factors such as limited noble metal resources, especially high cost of Pt, poor carbon monoxide (CO) tolerance, slow electron transfer kinetics, and instability of Pt based electro catalyst prompted the research for alternate electrode materials. Even though, noble metals could not be completely dispensed off as electrode materials, their utilization can be minimized. Pd based [12–15] anode catalysts are a possible alternative to Pt-based electro catalysts for DEFCs application. Pd has similar catalytic properties to that of Pt (both elements belong to the same group of the periodic table, with face-centered cubic (fcc) crystal structure and similar atomic size. Apart from this, factors such as low cost, superior electro catalytic activity and better resistance to the formation of intermediate species has been attracted to use Pd based catalyst ethanol oxidation reaction. Addition of non-noble metals in palladium catalyst to promote the catalytic activity and minimization of the use of noble metals [16,17]. Secondary elements such as Au [18–20], NiO [21], CeO_2 [22] and Ag [23] are added to noble metal electrode catalysts to improve the efficiency in DEFCs resulting from the bimetallic synergistic effect. Nickel oxide (NiO) plays the role of promoter along with the Pd nanoparticles during the ethanol oxidation reaction (EOR) in alkaline media. Nickel, in the form of $Ni(OH)_2$ and NiO are mostly used in a number of energy areas including Bio fuel, alcohol fuel cells, supercapacitors and electrochemical sensor applications because of their ability to catalyze reactions as well

* Corresponding author.
E-mail address: cmmagi@gmail.com (C. Mahendiran).

https://doi.org/10.1016/j.apsusc.2018.02.174
0169-4332/

as their higher natural abundance and low-cost [24–26]. Moreover, NiO has been used as co-catalyst to enhance the activity of Pd particles for electrooxidation of ethanol.Catalyst support materials should possess high electrical conductivity for the flow of electrons. Further, the material should have accessible surface area and chemical stability for improved performance of the supported catalyst. Carbon-based support materials like carbon black [27,28], carbon nanotubes (CNTs) [29–31] and rGO [32–34] have also been widely investigated. Among different electro catalyst supports, CNT based materials have unique identity due to their considerable electronic properties, high specific surface area and chemical stability. These unique properties make MWCNTs very useful as support material for metal nanoparticles (NPs). Analogous to CNTs, rGO is another allotrope of carbon (hexagonal lattice structure) with a few layer of carbon atoms is considered as one of the most useful materials in the current century because of its unique properties such as superior electrical conductivity, large surface area, excellent mechanical flexibility and high thermal/chemical stability [35,36]. Recently, hybrid materials such as MWCNTs/rGO [37], NiO/MWCNTs-rGO [38], PtRu/graphene-carbonnanotube [39] Graphene/MWCNTs/Fe_3O_4 [40] and Pd-Au(Cu)/rGO-CNTs [41] have also been employed as potential electrode materials for energy related applications.

The rGO supported Pd and Pd-based catalysts have also been developed as electro-catalysts for ethanol oxidation reaction. However, there are some problems with the use of rGO as a catalyst support. During the formation of rGO nanosheet, it tends to aggregate in solution due to π-π interactions between individual rGO sheets. This leads to lowering of surface area and conductivity [42]. This problem was surmounted in different ways, like surface modification of graphene, incorporation of metals and other carbon supports. The dispersion of nanoparticles (e.g., Pd, Pd-NiO) on MWCNTs may, to some extent, prevent the restacking of rGO during the catalyst preparation process. Carbon nanotubes decorated with metal nanoparticles incorporation between graphene sheets helps to prevent agglomeration [43,44] and also increases the specific surface area of graphene materials leading to enhancement of electronic conductivity. Hence, Pd-NiO/MWCNTs on rGO serves as novel catalyst support materials which enhances the catalytic activity of the nanoparticles as well as the electronic conductivity of graphene nanosheets. Also, the use of multiwalled carbon nanotubes ensures the utilization of high electrochemical surface area of rGO layers. Further it provides nano-channels of three-dimensional MWCNTs-rGO hybrid materials for enhanced and uniform distribution of active catalytic sites via surface functionalization.

In this present work, we report the facile synthesis of Pd and NiO nanoparticles anchored MWCNTs supported on rGO layers. The novel design has prevented the agglomeration of rGO, enhanced the electro catalytic activity and conductivity due to the availability of more active sites on MWCNT and rGO support. As synthesized Pd-NiO/MWCNTs/rGO electrocatalyst exhibits higher electrochemical ethanol oxidation activity when compared with Pd/MWCNTs/rGO and Pd/C catalysts due to the presence of NiO promoter along with Pd nanoparticle. In addition, high surface area provided by the rGO, facilitates the availability of more active sites and ensures their participation in the reaction.

2. Experimental

2.1. Materials

Natural Graphite Powder microcrystal grade (APS 2–15 μm micron; purity: 99.9995%) and Nickel nitrate hexahydrate [$Ni(NO_3)_2{\cdot}6H_2O$], Palladium chloride ($PdCl_2$), Sodium borohydride ($NaBH_4$) and Nafion resin (5 wt.% solution in aliphatic alcohols and water) were purchased from Sigma–Aldrich, India. Sulfuric acid (H_2SO_4, 97–98 wt.%), Hydrochloric acid (HCl, 37 wt.%), Ethanol (C_2H_5OH, 99.8 wt.%), Phosphoric acid (H_3PO_4 98 wt.%), Hydrogen peroxide (H_2O_2, 29–31 wt.%) and Potassium permanganate ($KMnO_4$, purity: 99.5) were purchased from Fischer chemicals, India.

2.2. Chemical vapor deposition method

Fig. 1 shows the chemical vapor deposition (CVD) method for the synthesis of MWCNTs using a bimetallic catalyst, acetylene, nitrogen and hydrogen gas. In a typical synthesis [45], 200 mg of Fe-Co/KIT-6 catalyst was placed in quartz boat inside the tubular furnace. The catalyst was purified with argon (Ar) gas at a flow rate of 110 mL min^{-1} for 30 min to remove water, and the metal particles were reduced by hydrogen (H_2) gas at a flow rate of 110 mL min^{-1} for 30 min. The carbon source, acetylene (C_2H_2) was sent in at a flow rate of 100 mL min^{-1} for 30 min through the furnace containing the catalyst at 800 °C. The tubular furnace was cooled to room temperature in Ar atmosphere. After completion of the MWCNTs growth process, the final product was obtained as black colored material. The impurities (silica, amorphous carbon) present in the synthesized material were removed by air oxidation process conducted at 450 °C for 2 h in a muffle furnace. Hydrofluoric acid (HF) treatment was carried out with 40% HF with stirring for 24 h at room temperature followed by filtering and washing with excess double distilled water. The obtained samples were further treated with nitric acid (10 wt.%) to remove the metal particles and washed with double distilled water. Finally, the material was dried at 100 °C for 5 h in an air atmosphere. The MWCNTs were functionalized with acid groups via treatment with a solution of nitric and sulfuric acids (1:3). 100 mg of MWCNTs were added to a 200 mL solution of sulfuric and nitric acids followed by ultrasound irradiation (ultrasonic processor PR-250) at 90 °C for 6 h at 500 rpm. The material was then filtered, washed thoroughly until the pH of the solution becomes neutral.

2.3. Graphene oxide synthesis

Graphene oxide (GO) was prepared from graphite powder using an improved Hummers' method [46] Solutions of concentrated H_2SO_4/H_3PO_4 (360:40 mL, 9:1 v/v), $KMnO_4$ (18.0 g, 6 wt equiv.) and 3.0 g of graphite flakes (1 wt equiv), were added gradually and heated to 60 °C for 12 h with continuous stirring. After cooling to room temperature, the mixture was poured into the cold water (400 mL) with 30% H_2O_2 (3 mL). Finally, the solid material washed with 200 mL of water, 200 mL of 10% HCl, and 200 mL of ethanol. For each wash, the mixture was filtered and centrifuged (6000 rpm for 4 h). The supernatant layer was separated by decantation. The solid obtained was dried under vacuum overnight at 65 °C to get Graphene oxide (GO).

2.4. Graphene oxide reduction

GO (100 mg) was dispersed in 100 mL of water followed by the addition of hydrazine hydrate (10 μL). The reaction mixture was refluxed at 80 °C for 1 h. The addition of hydrazine hydrate reduces the oxygen functional groups other than carboxyl groups present on the surface of GO. This selective process of removal of oxygen functionalities has been used to control the reduction of GO and their properties. Subsequently, $NaBH_4$ (1 mg) was added to reduce the carboxyl groups and other oxygen functional groups, if any, present on the GO surface. The resulting mixture was then refluxed for 36 h at 110 °C.

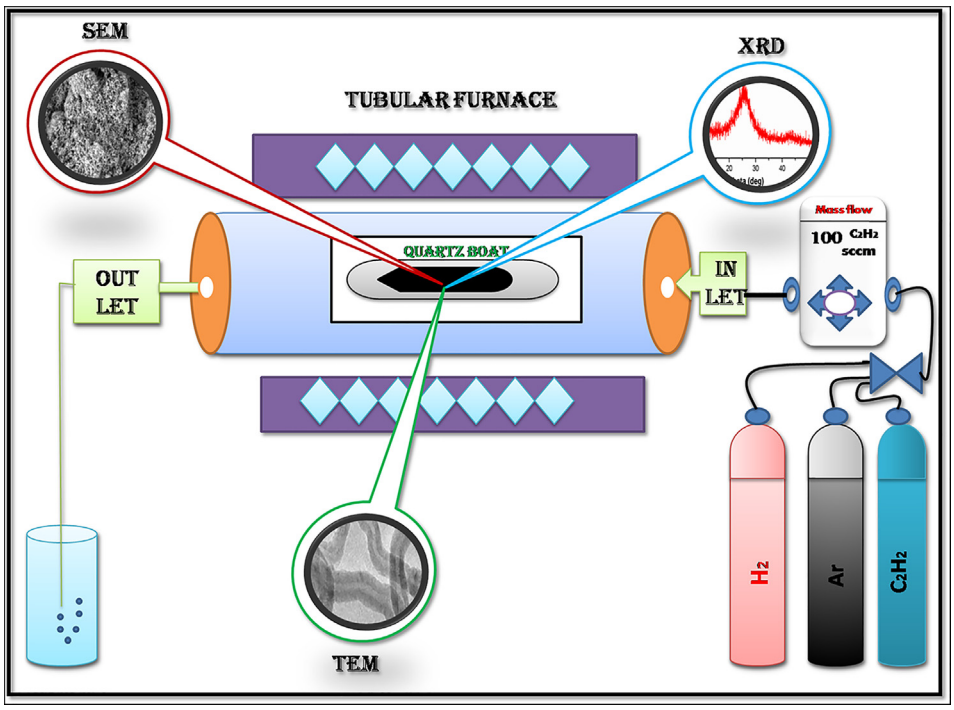

Fig. 1. Apparatus employed for the Chemical Vapour Deposition method (CVD).

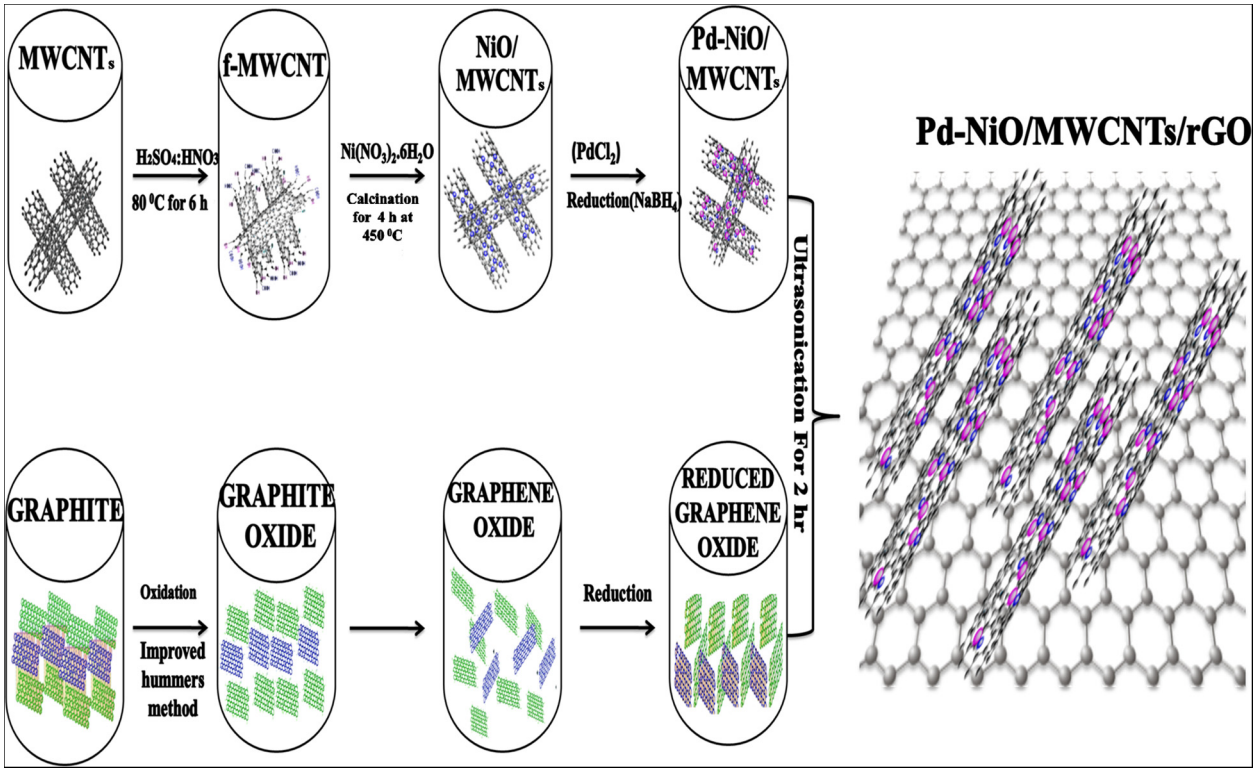

Fig. 2. Schematic representation of the method of synthesis of Pd-NiO/MWCNTs/rGO electrocatalyst.

2.5. Synthesis of Pd-NiO/MWCNTs/rGO electro catalyst

In a typical synthesis, appropriate amount of functionalized MWCNTs were dispersed in 50 mL de-ionized water using ultrasonication for 30 min. Then calculated amount of $Ni(NO_3)_2.6H_2O$ was added with constant stirring for 4 h at room temperature. The pH of the entire solution was adjusted to 10 by adding NaOH. The formed slurry was centrifuged, and thoroughly washed with deionized water and dried at 80 °C for 24 h in a vacuum oven. The material was calcined in air at 450 °C for 4 h in a tubular furnace and cooled to room temperature to obtain NiO/MWCNTs. According to the synthesis procedure

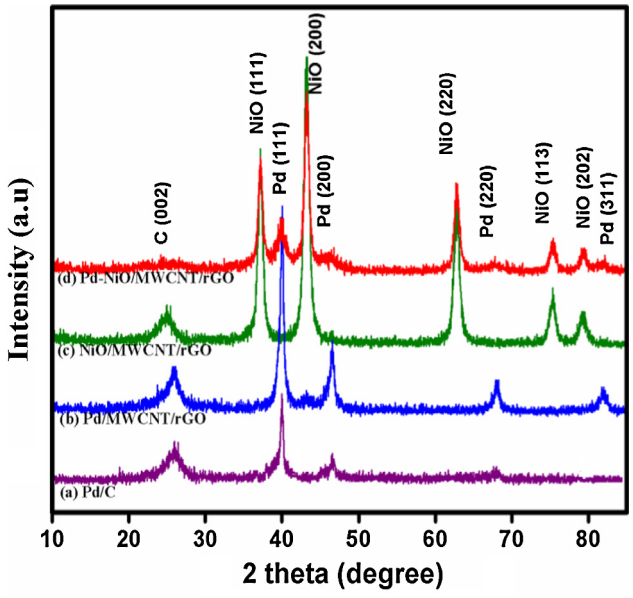

Fig. 3. (a) XRD patterns of Pd/C, (b) Pd/MWCNTs/rGO, (c) NiO/MWCNTs/rGO and (d) Pd-NiO/MWCNTs/rGO catalyst.

[47], calculated amount of $PdCl_2$ solution was added dropwise to NiO/MWCNTs nanocomposite under ultrasonication for 20 min. The resulting suspension was continuously stirred at 130 °C for 6 h. A freshly prepared solution of $NaBH_4$ (120 mg $NaBH_4$ dissolved in 10 mL water) reagent was added dropwise into the nanocomposite ($PdCl_2$-NiO/MWCNTs). The suspension was cooled to room temperature, centrifuged, and washed thoroughly with deionized water and dried at 80 °C for 12 h. Then, appropriate amount of rGO and as synthesized Pd-NiO/MWCNTs composites were dispersed in 100 mL of distilled water by ultrasonication (ultrasonic processor PR-250) for 2 h resulting in the formation of electrocatalyst, Pd-NiO-MWCNTs/rGO. Finally, the solid was filtered and washed several times with distilled water and ethanol, dried at 60 °C for 12 h in a vacuum oven. The same procedure was followed for the preparation of Pd-MWCNTs/rGO and NiO-MWCNTs/ rGO electrocatalysts. An equivalent proportion of rGO and MWCNTs (1:1) and 20 wt% of Pd were used for the synthesis of electrocatalyst. A schematic representation for the preparation of Pd-NiO/MWCNTs/rGO electrocatalyst is shown in Fig. 2.

2.6. Materials characterization

Powder X-ray diffraction (XRD) patterns of the materials were recorded within the 2θ angle range 10–90° at a scan rate of 0.5° min^{-1} using Rigaku Miniflex II diffractometer with CuKα as the radiation source at a wavelength of 0.154 nm. Scanning electron microscopy (SEM) and Energy Dispersive X-ray spectroscopy (EDX) (S-3400) were employed to carry out the surface morphology and metal loading ratio of the as-prepared electro catalysts, respectively. The HR-TEM images of the synthesized materials were recorded after dispersing the analytes in ethanol and placing

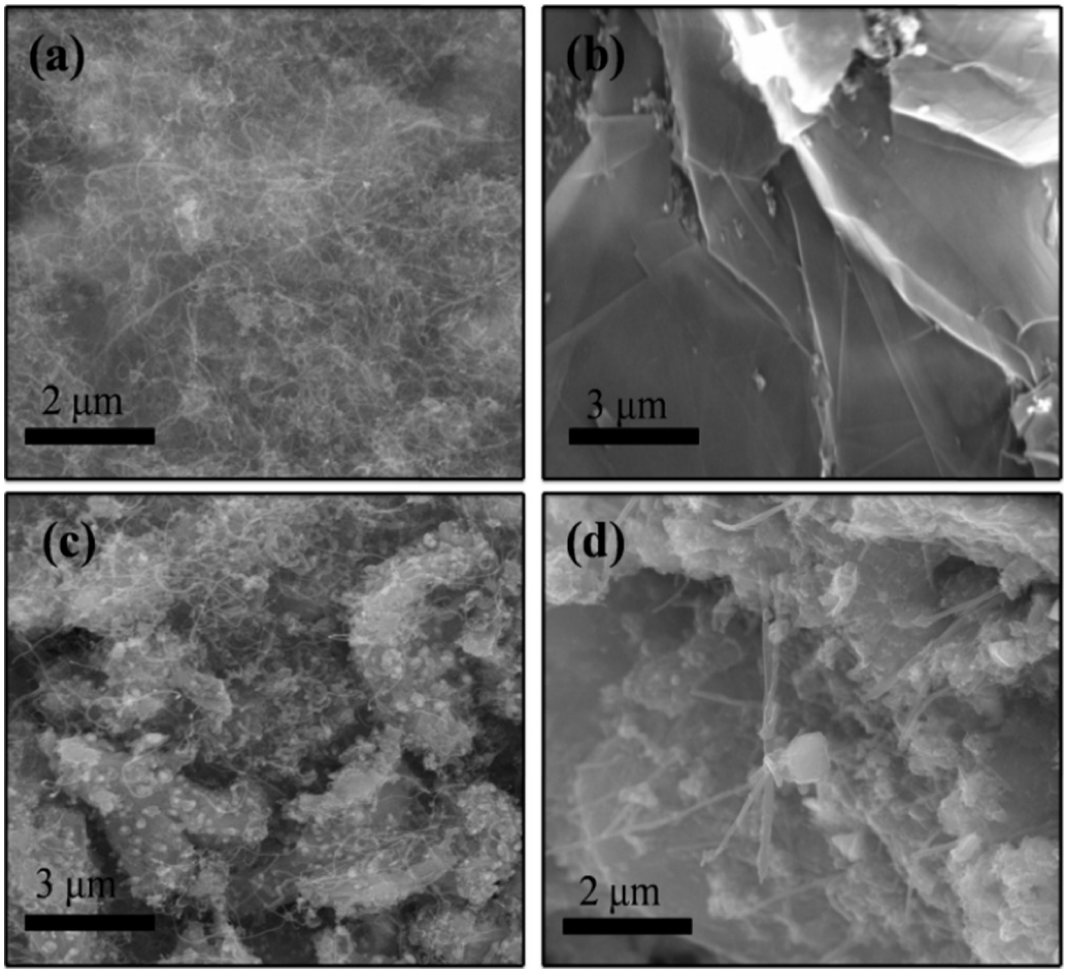

Fig. 4. (a) SEM images of MWCNTs, (b) rGO, (c) Pd-NiO/MWCNTs and (d) Pd-NiO/MWCNTs/rGO catalyst.

the same on a copper grid. The images were obtained by using JEOL JEM-2100 model, operating at an accelerating voltage of 100 kV. The surface composition of the materials was analyzed using X-ray photoelectron spectroscopy (XPS) using a Theta Probe Instrument (Omicron Nanotechnology spectrometer with hemispherical analyzer). The monochromatized Mg KαX-source (E = 1253.6 eV) was operated at 15 kV and 20 mA.

2.7. Electrochemical measurement

The working electrode coated with nanocatalyst was prepared by the following procedure [48]. Glassy Carbon Electrode (GCE) (3 mm) was carefully polished with 0.05 μm alumina powder prior to each experiment. For the electrode preparation, 2.5 mg of electrocatalyst was ultrasonically mixed with 200 μL of ethanol, followed by ultrasonication of the suspension for 30 min to acquire a homogeneous mixture. Calculated quantity of prepared catalyst ink was dropped onto the top of the GCE surface using micropipette followed by drying at room temperature. Finally, the catalyst was covered with Nafion solution (5 wt.%) to ensure that the catalyst was tightly attached to the electrode surface. The Pd-NiO/MWCNTs/rGO electro catalyst deposited on the GC surface was used as the working electrode for the electro oxidation of ethanol.

The electrochemical properties of materials were carried out in a conventional three-electrode cell connected to an electrochemical analyzer (Biologic SB-150). The electrochemical system consists of three electrode setups which are glassy carbon used as working electrode, the silver chloride (Ag/AgCl) employed as a reference electrode and the platinum electrode was used as counter electrode. The electrochemical experiments were carried out at room temperature in 1 M KOH and 1 M C_2H_5OH used as supporting electrolyte.

3. Results and discussion

3.1. Structure of electrocatalysts and catalyst supports – XRD analysis

The structural information for Pd/C, Pd/MWCNT/rGO, NiO-MWCNT/rGO and Pd-NiO/MWCNT/rGO catalysts were determined by XRD, and the diffractograms are shown in Fig. 3. From the XRD pattern of different catalysts, specialty peaks were noticed at 2θ = 25.95, 37, 40, 43.15, 46.8, 62, 68, 67, 75.40, 79.20 and 82°.

Fig. 3a shows the initial peak at a 2θ value of 26°and is referred to carbon (0 0 2) plane. The first isolated peaks in Fig. 3(b, c and d) corresponding to graphitic structure of MWCNTs and rGO due to hexagonal arrangement of carbon atoms [49a]. The XRD profiles (Fig. 3(a, b and d)) show typical diffraction peaks at 40, 46.8, 68, and 82° attributable to the characteristic (1 1 1), (2 0 0), (2 2 0) and (3 1 1) [48] planes of palladium corresponds to face-centered cubic structure (fcc). The presence of NiO was confirmed from the observation of X-ray diffraction peaks at 37, 43.15, 62.5, 75.40 and 79.20° corresponding to (1 1 1), (2 0 0), (2 2 0), (1 1 3) and (2 0 2) [16,50] crystal planes Fig. 3c–d. The XRD pattern of Ni^0 was not observed which was due to the instability of Ni^0 which readily converts to NiO. The Pd–NiO/MWCNTs/rGO electrocatalyst Fig. 3d indicates that the diffraction peak at 2θ = 26° is relatively low, which perhaps indicates that the significant face-to-face

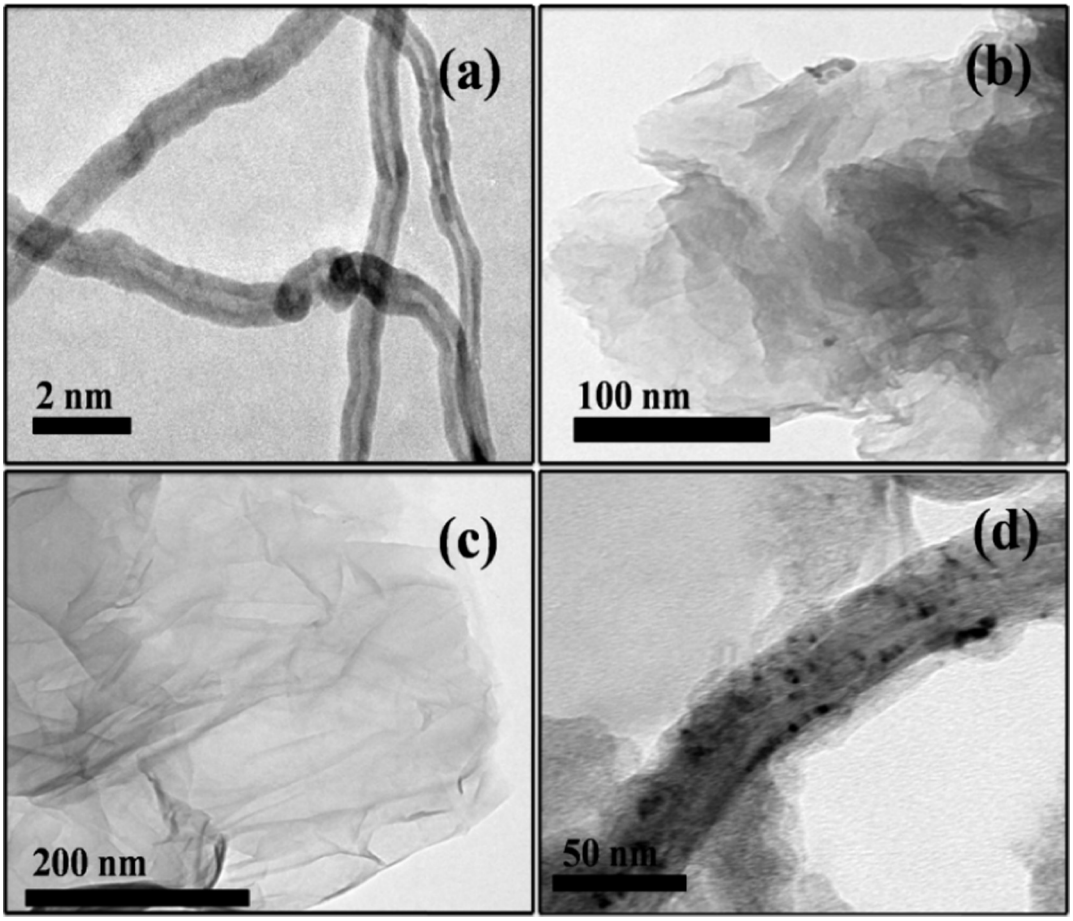

Fig. 5. (a) TEM images of MWCNTs, (b) GO, (c) rGO, (d) Pd-NiO/MWCNTs catalyst.

stacking is absent due to the introduction of Pd-NiO/MWCNTs composite on the surface of rGO nanosheets [10,49b]. Average particle sizes of Pd in Pd–NiO/MWCNT/rGO and Pd/C electro catalysts were calculated using Debey-Scherrer formula which were found to be 4.2 and 3.5 nm respectively.

$$d = 0.9\lambda/B_{2\theta}\cos\theta_{max} \quad (1)$$

Typical XRD patterns of graphite, GO [51], rGO and MWCNTs Fig. S1 were provided in the electronic supplementary information (ESI).

3.2. Morphology of electro catalysts and catalyst supports

The surface morphologies of MWCNTs, rGO, Pd-NiO/MWCNTs, and Pd-NiO/MWCNTs/rGO are depicted in Fig. 4. The formation of MWCNTs without any major contamination Fig. 4a reveals the purity of carbon nanotubes. Randomly aggregated thin, crumpled sheets of rGO are shown in Fig. 4b [52,53]. Uniform dispersion of Pd-NiO nanoparticle on the surface of MWCNT in Pd-NiO/MWCNT electrocatalyst was observed from SEM image Fig. 4c. SEM micrograph of the Pd-NiO/MWCNTs/rGO electrocatalyst provides the evidence for the presence of well dispersed Pd and NiO nanoparticles on MWCNTs which were decorated on rGO Fig. 4d. The presence of Pd-NiO/MWCNTs nanocomposite on the surface of rGO prevents aggregation of rGO nanosheets.

The structure, composition and the distribution of the metallic and metal oxide nanoparticles in the Pd-NiO/MWCNTs/rGO electrocatalyst were further examined by HR-TEM and EDX analysis and the results are provided in Figs. 5 and 6 respectively. For comparison, the TEM images of MWCNTs, GO, rGO and Pd-NiO/MWCNT are shown in Fig. 5a-d respectively. Nanotubular structures with interlace twisted tubes were observed Fig. 5a [43]. In comparison with rGO, GO appeared to accumulate more layers [52] as shown in Fig. 5b and c. Uniform dispersion of Pd and NiO nanoparticles functionalized MWCNTs were observed in the Fig. 5d. HR-TEM image of Pd-NiO/MWCNTs/rGO depicted the crystalline nature of the nanoparticles of Pd and NiO as shown in Fig. 6a. Presence of polycrystalline particles of NiO and Pd in Pd-NiO/MWCNTs/rGO electrocatalyst were confirmed from HRTEM analysis wherein the particles with an interlayer spacing of 0.238 and 0.317 nm for NiO and Pd respectively, were observed Fig. 6b. It demonstrates that the Pd-NiO nanoparticles strongly interact and spread widely on the MWCNTs. Perhaps, the strong interaction between rGO surface with the Pd-NiO/MWCNTs composites, prevent the aggregation and growth of the nanoparticles to form ample particles. Elemental analysis of the Pd-NiO/MWCNTs/rGO electrocatalyst was carried out by EDX and the corresponding spectrum is given in Fig. 6c. The Pd-NiO/MWCNTs/rGO electrocatalyst are composed of C, O, Ni, and Pd. Cu signal arises from the stub on which the analyte was loaded for EDX analysis.

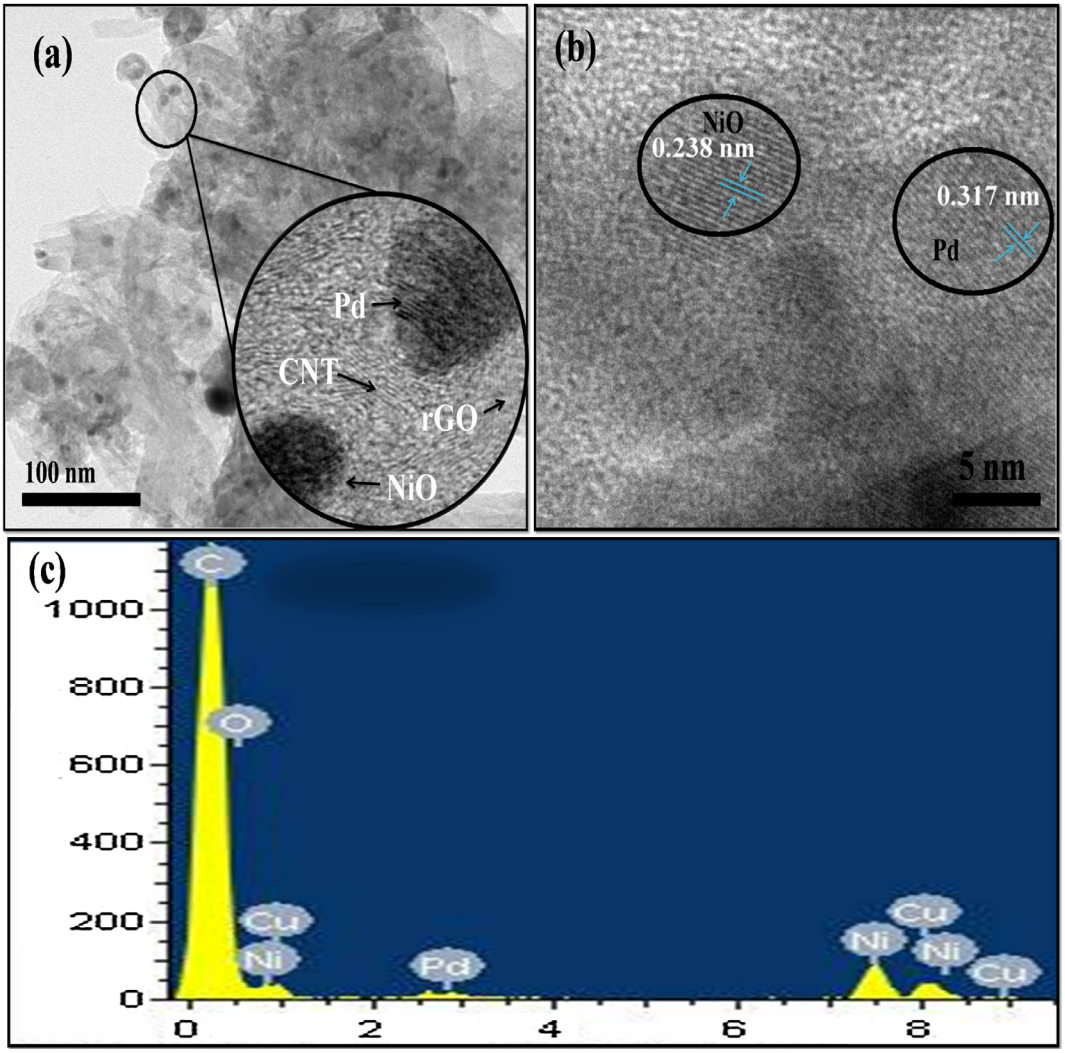

Fig. 6. (a) HR-TEM images of Pd-NiO/MWCNTs/rGO, (b) Fringes of Pd and NiO in Pd-NiO/MWCNTs/rGO catalyst, (c) EDX spectrum of Pd-NiO/MWCNTs/rGO catalyst.

3.3. XPS analysis

X-ray photoelectron spectroscopy (XPS) study revealed the chemical properties of Pd-NiO/MWCNTs/rGO electrocatalyst. Fig. 7a shows the XPS survey of Pd-NiO catalyst on MWCNTs and rGO supports. The elemental survey scan contained the atomic peaks of (C 1s) carbon, (O 1s) oxygen, (Pd 3d) palladium and (Ni 2p) Nickel Oxide. Three de-convoluted peaks around 284.7, 288.7 and 286.1 eV corresponding to C—C, O—C=O and C—O [54] of C1s spectra of MWCNTs/rGO were observed Fig. 7b. XPS spectra of Pd $_{3d}$ and Ni $_{2p}$ were also recorded Fig. 7c to illustrate the valence state of the elements. Pd_{3d} region of the XPS spectrum of the Pd-NiO/MWCNTs/rGO electrocatalyst is displayed in Fig. 7c. A doublet containing a high-energy band at 340.12 eV and a low-energy band at 335.25 eV correspond to $Pd3d_{3/2}$ and $Pd3d_{5/2}$ [55] were observed. The spin-orbit coupling in nickel-based mixture is responsible for the peak in the region of 870–885 eV typical of Ni $2P_{1/2}$. The peak appeared to develop at 850 to 869 eV [56,57] was due to the additional intense Ni $2P_{3/2}$ signal Fig. 7d.

3.4. Electrochemical catalytic activity

The electrochemical behavior of Pd-NiO/MWCNTs/rGO, Pd/MWCNTs/rGO and Pd/C electrocatalysts were studied using cyclic voltammetry (CV). The electrochemical performance of Pd-NiO/MWCNTs/rGO, Pd/MWCNTs/rGO and Pd/C modified electrodes was evaluated in 1 M KOH in the potential window of −1 to 0.20 V, and the corresponding cyclic voltammograms are displayed in Fig. 8a. The CV pattern was attributed to hydroxide (OH^-) adsorption/desorption on the surface of Pd. The anodic potential sweep entails in two ways which are the adsorption of hydrogen and oxidation of Pd to PdO [58]. The hydrogen adsorption takes

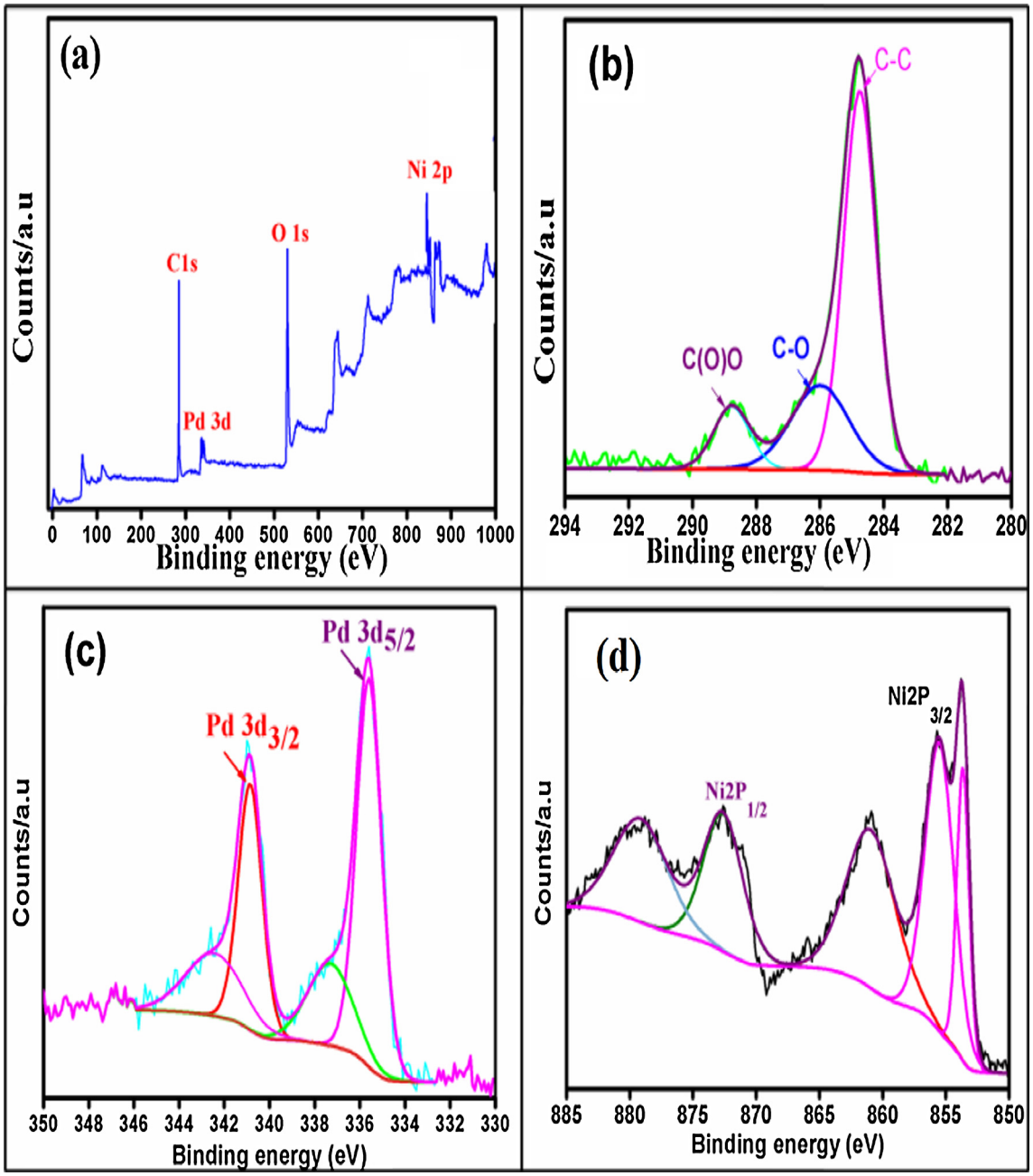

Fig. 7. XPS spectra of Pd-NiO/MWCNTs/rGO catalyst showing (a) elemental scan survey, (b) C 1s, (c) Pd 3d and (d) Ni 2p regions.

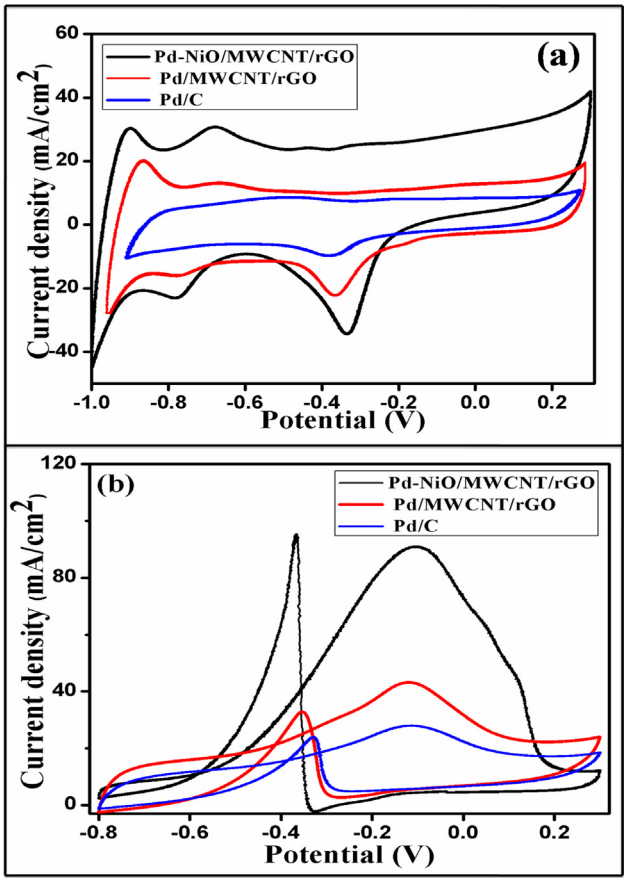

Fig. 8. (a) Cyclic voltammograms of Pd/MWCNTs/rGO, Pd-NiO/MWCNTs/rGO and Pd/C electrodes in 1.0 M KOH solution and (b) cyclic voltammograms of ethanol oxidation on Pd/MWCNTs/rGO, Pd-NiO/MWCNTs/rGO and Pd/C electrodes.1.0 M KOH + 1.0 M Ethanol. scan rate: 20 mV s^{-1}.

place at about −0.9 to −0.5 V, while it is still uncertain with the potential −0.35 V region of PdO to Pd in alkaline conditions. However, it has been suggested that PdO formation occurs at more positive potentials. The regeneration of Pd surface by the reduction of PdO to Pd occurs in the range of −0.2 to −0.45 V [14]. The electro catalytic activity depends on electrochemical active surface area (EASA). The EASA [59–61] has been measured by reduction of PdO in the as synthesized catalyst from the equation: EASA = Q/SI, where Q is the coulombic charge in mC, S is the proportionality constant and I is the loading of electrocatalyst (g) on GC electrode. Pd-NiO/MWCNTs/rGO exhibited the highest active surface area (42.65 m^2/g), compared to Pd/MWCNTs/rGO (21.62 m^2/g) and Pd/C (15.69 m^2/g) as showed in Fig. 8a. The mass activity (MA) of Pd-NiO/MWCNTs/rGO, Pd-MWCNTs/rGO and Pd/C catalysts are 101.6 mA/mg, 48.38 mA/mg and 33.88 mA/mg respectively and their corresponding specific activity (SA) are 0.23 mA cm^{-2}, 0.22 mA cm^{-2} and 0. 21 mA cm^{-2}.

The catalytic behavior of the Pd-NiO/MWCNTs/rGO electrocatalyst for ethanol oxidation reaction with 1 M ethanol in 1 M KOH was evaluated using two protruding curves in the cyclic voltammetery. The ethanol oxidation curves on the Pd/C, Pd/MWCNTs/rGO, and Pd-NiO/MWCNTs/rGO electrocatalysts are presented in Fig. 8b. Two characteristic peaks were found in the cyclic voltammograms: (i) anodic sweep potential range of −0.2 to 0.0 V and (ii) cathodic sweep potential range of −0.2 to −0.4 V. The EOR on Pd in alkaline media was proposed with the following reaction mechanism [8,15].

$$Pd + CH_3CH_2OH \rightarrow Pd - CH_3CO_{ads} + 3H_2O + 3e^- \quad (2)$$

$$Pd + OH \rightarrow Pd - OH_{ads}e^- \quad (3)$$

$$Pd - CH_3CO_{ads} + Pd - OH_{ads} \rightarrow Pd - CH_3COOH + Pd \quad (4)$$

$$Pd - CH_3COOH + OH^- \rightarrow Pd + CH_3COO^- + H_2O \quad (5)$$

The CH_3CO or other carbonaceous reactive intermediates will strongly get adsorbed on the surface of Pd and block the active sites (Eq. (2)). In the region starting from −0.7 V, Pd begins to adsorb OH^-. With the adsorption of OH^- species on Pd, the strongly adsorbed carbonaceous species will be quickly stripped away, resulting in an increased current density (Eq. (3) and (4)) [62] as shown in the Fig. 8b. It can be seen that the electrocatalytic activity in the oxidation of acetaldehyde is the highest, while no oxidation current is drawn from the acetate solution. This suggests that acetate is the final product and acetaldehyde is an active intermediate in EOR on Pd electrode. The amount of Pd loading of the electrode and the observed current density were used to determine the elctrocatalytic activity of the electrodes used for electrooxidation of ethanol. In this case, the Pd-NiO/MWCNTs/rGO electrocatalyst shows the highest electro catalytic activity among the three catalysts examined in the present study. The observed electrocatalytic activity of the Pd-NiO/MWCNTs/rGO electrocatalyst is (90.89 mA/cm^2), which is two times higher than Pd/MWCNTs/rGO (43.50 mA/cm^2) and three times higher than Pd/C (28.0 mA/cm^2) commercial catalyst. The results showed that the rGO support is effective since it facilitate for easy electron charge transfer access to prevent agglomeration of rGO sheets and metal-metal oxide nanoparticles as illustrated in TEM analysis Fig. 6a. This can be due to the presence of oxygen-rich functional groups on MWCNTs, which act as nucleation sites for metal particles during the synthesis. Indeed, there could be a better dispersion of the metal particles, greater active surface area and better interaction between both metal species [63,64]. The electrochemical activity of Pd-NiO/MWCNTs/rGO electrocatalyst was compared with other catalysts and the corresponding results are presented in (ESI) Table 1.

Further, a study of ethanol oxidation reaction (EOR) was carried out for catalysts in basic media by linear sweep voltammograms (LSVs) at a scan rate of 20 mV s^{-1} in 1.0 M C_2H_5OH and 1.0 M KOH in the potential window of −0.7 to 0.20 V using the same catalysts. The linear relationship indicates the diffusion controlled behavior of all prepared electrocatalysts and the slow scan rate minimizes the mass transfer issues. The quasi-steady state curve for the ethanol electro-oxidation reaction (EOR) is shown in Fig. 9. The figure shows that the Pd-NiO/MWCNTs/rGO electrocatalysts are found to increase the current density and the potential values show a shift to negative values. The surface modification also affects the onset potential. The onset potential of Pd-NiO/MWCNTs/rGO electrocatalyst, is remarkably lower than that of Pd/MWCNTs/rGO and Pd/C.

Chronoamperometry (CA) was used to study the effect of the support on the activity of catalysts and stability of ethanol oxidation reaction Fig. 10. A constant potential of −0.1 V was applied to the working electrode for 3500 s. The working electrode was immersed in a solution containing 1.0 M C_2H_5OH in 1.0 M KOH. Due to initial oxidation of ethanol, all curves began with the decreasing current density at the start up. The Pd-NiO/MWCNTs/rGO electrocatalyst showed good stability and excellent electro catalytic activity which is higher than Pd/MWCNTs/rGO and Pd/C. The supports, MWCNTs and rGO, not only facilitated the effective distribution of Pd and NiO nanoparticles but also directed the appropriate geometric distribution of the electrocatalytic active species that were easily accessible for the adsorption of ethanol molecules and their subsequent electrooxidation. Thus, Pd-NiO/MWCNTs/rGO electrocatalyst

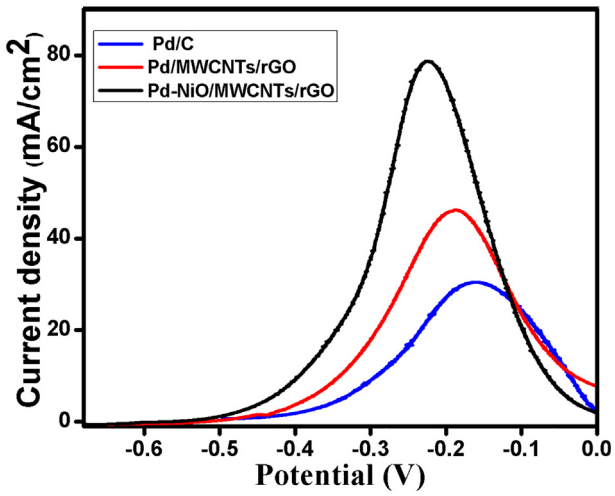

Fig. 9. Linear sweep voltammograms for ethanol oxidation Pd/MWCNTs/rGO, Pd-NiO/MWCNTs/rGO and Pd/C catalyst in 1 M KOH and 1.0 M Ethanol. Scan rate 20 mV $s^{-1.}$

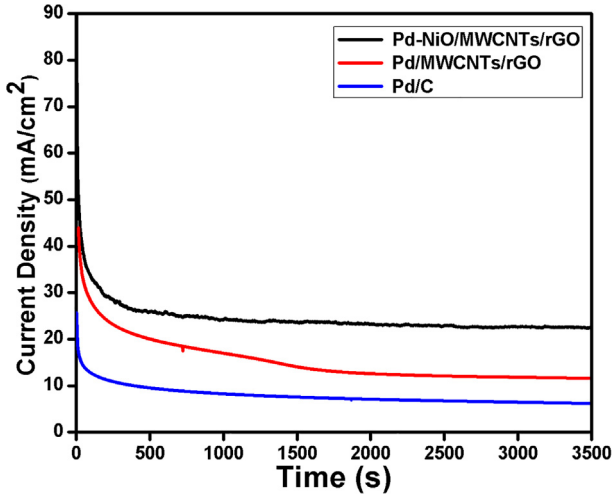

Fig. 10. Chronoamperometric curves of Pd/MWCNTs/rGO, Pd-NiO/MWCNTs/rGO and Pd/C at −0.1 V in 1.0 M KOH + 1.0 M Ethanol.

exhibited the highest electrode stability. The enhanced stability is due to the carboxylic functional groups attached on MWCNTs surface which enabled the interaction between metals and MWCNTs support. Also, the high crystallinity of the rGO provided a good electrical connection at molecular level.

4. Conclusions

In summary, Pd-NiO/MWCNTs/rGO electrocatalyst was successfully synthesized by two-step strategy and the catalytic properties were investigated for electrooxidation of ethanol in an alkaline medium. As synthesized electrocatalyst were characterized using XRD, HR-TEM, EDX and XPS analysis methods. HR-TEM results indicate that fine dispersion of Pd-NiO nanoparticles on the surface of MWCNTs and rGO supports. Electrochemical analysis results shows, Pd-NiO/MWCNTs/rGO exhibit higher tolerance, high electrochemical stability and activity than Pd/MWCNTs/rGO and Pd/C catalysts for electrooxidation of ethanol. The synergistic effect derived from the bimetal combination of Pd-NiO NPs which resides on MWCNT and rGO, is also known to resist the poisoning of reaction sites during the electrooxidation process and thereby leading to improved stability as shown by CA study. In addition, MWCNTs act as a good promoter and pore producer in rGO support to increase the mass transport of ethanol. This phenomenal enhancement of the electro catalytic performance contributes to a new perception into the MWCNTs and rGO supported metallic systems for electrooxidation of ethanol in alkaline medium.

Acknowledgements

The corresponding author would like to thank DST (India)-SERB for the sanction of this project (CS-257/2014) and financial support under Start-Up research grant (Young scientists).

Appendix A. Supplementary material

Supplementary data associated with this article can be found, in the online version, at https://doi.org/10.1016/j.apsusc.2018.02.174.

References

[1] L. Lin, W. Sheng, S. Yao, D. Ma, G. Jingguang, Pt/MO_2C/C as a highly active and stable catalyst for ethanol electrooxidation, J. Power Sources 345 (2017) 182–189.
[2] M.D. Obradovic, Z.M. Stancic, U.C. Lacnjevac, V.V. Radmilovic, A. Gavrilovic-Wohlmuther, V.R. Radmilovic, S.Lj. Gojkovic, Electrochemical oxidation of ethanol on palladium-nickel nanocatalyst in alkaline media, Appl. Catal. B Environ. 189 (2016) 110–118.
[3] K. Ding, Y. Li, Y. Zhao, J. Zhao, Y. Chen, Q. Wang, Preparation of a trimetallic Pd1NiyAl0.5 composite nanoparticle by a hydrothermal method for ethanol oxidation reaction, Int. J. Electrochem. Sci. 10 (2015) 8844–8857.
[4] R.M. Abdel Hameed, Facile preparation of Pd-metal oxide/C electrocatalysts and their application in the electrocatalytic oxidation of ethanol, Appl. Surf. Sci. 411 (2017) 91–104.
[5] S. Jongsomjit, K. Sombatmankhongc, P. Prapainainar, Effect of acid functionalised carbon supports for Pd–Ni–Sn catalyst on ethanol oxidation reaction, RSC Adv. 5 (2015) 61298.
[6] S. Song, P. Tsiakaras, Recent progress in direct ethanol proton exchange membrane fuel cells (DE-PEMFCs), Appl. Catal. B 63 (2006) 187–193.
[7] Claude Lamy, Alexandre Lima, Vernique Lerhun, F. Delime, C. Coutanceau, J.-M. Leger, Recent advanced in the development of direct alcohol fuel cells (DAFC), J. Power Sources 105 (2002) 283–296.
[8] K. Ding, Y. Zhao, L. Liu, Y. Cao, Q. Wang, H. Gu, X. Yan, Z. Guo, Pt-Ni bimetallic composite nanocatalysts prepared by using multi-walled carbon nanotubes as reductants for ethanol oxidation reaction, Int. J. Hydrogen Energy 39 (2014) 17622–17633.
[9] P. Mukherjee, J. Bagchi, S. Dutta, S. Kumar Bhattacharya, The nickel supported platinum catalyst for anodic oxidation of ethanol in alkaline medium, Appl. Catal. A 506 (2015) 220–227.
[10] V. Comignani, J.M. Sieben, M.E. Brigante, M.M.E. Duarte, Carbon supported Pt-NiO nanoparticles for ethanol electro-oxidation in acid media, J. Power Sources 278 (2015) 119–127.
[11] J.E. Sulaiman, S. Zhu, Z. Xing, Q. Chang, M. Shao, Pt−Ni octahedra as electrocatalysts for the ethanol electro- oxidation reaction, ACS Catal. 7 (2017) 5134–5141.
[12] L. Chen, L. Lu, H. Zhu, Y. Chen, Y. Huang, Y. Li and L. Wang, Improved ethanol electrooxidation performance by Shortening Pd–Ni active site distance in Pd–Ni–P nanocatalysts, Nat. Commun. doi: 10.1038/ncomms14136.
[13] Z.X. Liang, T.S. Zhao, J.B. Xu, L.D. Zhu, Mechanism study of the ethanol oxidation reaction on palladium in alkaline media, Electrochim. Acta 54 (2009) 2203–2208.
[14] J. Zhong, D. Bin, B. Yan, Y. Feng, K. Zhang, J. Wang, C. Wang, Y. Shiraishi, P. Yang, Y. Du, Highly active and durable flowerlike Pd/Ni(OH)2 catalyst for the electrooxidation of ethanol in alkaline medium, RSC Adv. (2016), https://doi.org/10.1039/C6RA14321K.
[15] L.P.R. Moraes, B.R. Matos, C. Radtke, E.I. Santiago, F.C. Fonseca, S.C. Amico, C.F. Malfatti, Synthesis and performance of palladium-based electrocatalysts in alkaline direct ethanol fuel cell, Int. J. Hydrogen Energy. 41 (2016) 6457–6468.
[16] S.S. Hossain, J. Saleem, A. Al. Ahmed, M.M. Hossain, M.N. Shaikh, S.U. Rahman, G. Mc Kay, Preparation and evaluation of nickel oxide-carbon nanotube supported palladium as anode electrocatalyst for formic acid fuel cells, Int. J. Electrochem. Sci. 11 (2016) 2686–2708.
[17] L. Li, M. Chen, G. Huang, N. Yang, L. Zhang, H. Wang, Yu. Liu, Wei Wang, J. Gao, A green method to prepare Pd-Ag nanoparticles supported on reduced graphene oxide and their electrochemical catalysis of methanol and ethanol oxidation, J. Power Sources 263 (2014) 13–21.
[18] Z. Huang, H. Zhou, C. Li, F. Zeng, C. Fua, Y. Kuang, Preparation of well-dispersed PdAu bimetallic nanoparticles on reduced graphene oxide sheets with excellent electrochemical activity for ethanol oxidation in alkaline media, J. Mater. Chem. 22 (2012) 1781.

[19] J.B. Xu, T.S. Zhao, S.Y. Shen, Y.S. Li, Stabilization of the palladium electrocatalyst with alloyed gold for ethanol oxidation, Int. J. Hydrogen Energy 35 (2010) 6490–6500.
[20] Y. Tao, A. Dandapat, L. Chen, Y. Huang, Y. Sasson, Z. Lin, J. Zhang, L. Guo, T. Chen, Pd-on-Au supra-nanostructures decorated graphene oxide: an advanced electrocatalyst for fuel cell application, Langmuir 32 (2016) 8557–8564.
[21] A. Dutta, J. Datta, Energy efficient role of Ni/NiO in PdNi nano catalyst used in alkaline DEFC, J. Mater. Chem. A. 2 (2014) 3237.
[22] Q. Tan, C. Du, Y. Sun, G. Yin, Y. Gao, Pd-around-CeO2 hybrid nanostructure catalyst: three-phase-transfer synthesis, electrocatalytic properties and dual promoting mechanism, J. Mater. Chem A. 2 (2014) 1429–1435.
[23] K. Kakaei, M. Dorraji, One-pot synthesis of Palladium Silver nanoparticles decorated reduced graphene oxide and their application for ethanol oxidation in alkaline media, Electrochim. Acta 14 (S0013-4686) (2014), 01556-4.
[24] Y. Miao, L. Ouyang, S. Zhou, L. Xu, Z. Yang, M. Xiao, R. Ouyang, Electrocatalysis and electroanalysis of nickel its oxides hydroxides and oxyhydroxides toward small molecules, Biosens. Bioelectron. 53 (2014) 428–439.
[25] C. Xua, P.K. Shen, Y. Liu, Ethanol electrooxidation on Pt/C and Pd/C catalysts promoted with oxide, J. Power Sources 164 (2007) 527–531.
[26] C. Xua, Z. Tian, P. Shen, S.P. Jiang, Oxide (CeO_2, NiO, Co3O4 and Mn3O4)-promoted Pd/C electrocatalysts for alcohol electrooxidation in alkaline media, Electrochimica Acta 53 (2008) 2610–2618.
[27] F. Hu, C. Chen, Z. Wang, G. Wei, P. Kang, Shen, Mechanistic study of ethanol oxidation on Pd–NiO/C electrocatalyst, Electrochim. Acta 52 (2006) 1087–1091.
[28] R.M. Modibedi, T. Mehlo, K.I. Ozoemena, M.K. Mathe, Preparation, characterisation and application of Pd/C nanocatalyst in passive alkaline direct ethanol fuel cells (ADEFC), Int. J. Hydrogen Energy. 40 (2015) 15605–15612.
[29] Y. Wang, Q. He, K. Ding, H. Wei, J. Guo, Q. Wang, R. Connor, X. Huang, Z. Luo, T. D. Shen, S. Wei, Z. Guoa, Multiwalled carbon nanotubes composited with palladium nanocatalysts for highly efficient ethanol oxidation, J. Electrochem. Soc. 162 (7) (2015) F755–F763.
[30] S. Jongsomjit, K. Sombatmankhong, P. Prapainainar, Effect of acid functionalised carbon supports for Pd–Ni–Sn catalyst on ethanol oxidation reaction, RSC Adv. 5 (2015) 61298–61308.
[31] C. Mahendiran, D. Rajesh, T. Maiyalagan, K. Prasanna, Pd nanoparticles-supported carbon nanotube-encapsulated NiO/MgO composite as an enhanced electrocatalyst for ethanol electrooxidation in alkaline medium, Chem. Select 2 (2017) 11438–11444.
[32] F. Ren, H. Wang, C. Zhai, M. Zhu, R. Yue, Y. Du, P. Yang, J. Xu, W. Lu, Clean method for the synthesis of reduced graphene oxide- supported PtPd alloys with high electrocatalytic activity for ethanol oxidation in alkaline medium, ACS Appl. Mater. Inter faces. 6 (2014) 3607–3614.
[33] J.L. Tan, A.M. De Jesus, S.L. Chua, J. Sanetuntikul, S. Shanmugam, B.J.V. Tongol, H. Kim, Preparation and characterization of palladium-nickel on grapheneoxide support as anode catalyst for alkaline direct ethanol fuel cell, Appl. Catal. A 531 (2017) 29–35.
[34] S. Kabir, A. Serov, K. Artyushkova, P. Atanassov, Design of novel graphene materials as a support for palladium nanoparticles highly active catalysts towards ethanol electrooxidation, Electrochim. Acta 203 (2016) 144–153.
[35] S. Stankovich, D.A. Dikin, G.H.B. Dommett, K.M. Kohlhaas, E.J. Zimney, E.A. Stach, R.D. Piner, S.T. Nguyen, R.S. Ruoff, Graphene based composite materials, Nature (2006), 442-20.
[36] A.K. Geim, K.S. Novoselov, The rise of graphene, Nat. Mater. (2007) 6.
[37] B.P. Vinayan, R. Nagar, V. Raman, N. Rajalakshmi, K.S. Dhathathreyan, S. Ramaprabhu, Synthesis of graphene-multiwalled carbon nanotubes hybrid nanostructure by strengthened electrostatic interaction and its lithium ion battery application, J. Mater. Chem. 22 (2012) 9949.
[38] R. Prasad, V. Ganesh, B.R. Bhat, Nickel-oxide multiwall carbon-nanotube/reduced graphene oxide a ternary composite for enzyme-free glucose sensing, RSC Adv. 00 (2016) 1–3.
[39] Y.S. Wang, S.Y. Yang, S.M. Li, H.W. Tien, S.T. Hsiao, W.H. Liao, C.H. Liu, K.H. Chang, C.C.M. Ma, C.C. Hu, Three-dimensionally porous graphene–carbon nanotube composite-supported PtRu catalysts with an ultrahigh electrocatalytic activity for methanol oxidation, Electrochim. Acta 87 (2013) 261–269.
[40] R.B. Song, C.E. Zhao, L.P. Jiang, E.S. Abdel-Halim, J.R. Zhang, J.J. Zhu, Bacteria-affinity 3D macroporous graphene/MWCNTs/Fe_3O_4 foams for high-performance microbial fuel cells, ACS Appl. Mater. Interfaces 8 (2016) 16170–16177.
[41] M. Wanga, Z. Maa, R. Lia, B. Tanga, X.Q. Baob, Z. Zhangc, X. Wanga, Novel flower-like PdAu(Cu) anchoring on a 3D rGO-CNT sandwich-stacked framework for highly efficient methanol and ethanol electro-oxidation, Electrochim. Acta 227 (2017) 330–344.
[42] D. Li, M.B. Muller, S. Gilje, R.B. Kaner, G.G. Wallace, Processable aqueous dispersions of graphene nanosheets, Nat. Nanotechnol. 3 (2008).
[43] R.I. Jafri, T. Arockiados, N. Rajalakshmi, S. Ramaprabhua, Nanostructured Pt dispersed on graphene-multiwalled carbon nanotube hybrid nanomaterials as electrocatalyst for PEMFC, J. Electrochem. Soc. 157 (2010), 6-B874-B879.
[44] Q. Cheng, J. Tang, J. Ma, H. Zhang, N. Shinyaa, L.C. Qinc, Graphene and carbon nanotube composite electrodes for supercapacitors with ultra-high energy density, Phys. Chem. Chem. Phys. 13 (2011) 17615–17624.
[45] J. Balamurugan, A. Pandurangan, R. Thangamuthu, Growth of well graphitized MWCNTs over novel 3D cubic bimetallic KIT-6 towards the development of an efficient counter electrode for dye-sensitized solar cells, Org. Electron. 14 (2013) 1833–1843.
[46] D.C. Marcano, D.V. Kosynkin, J.M. Berlin, A. Sinitskii, Z. Sun, A. Slesarev, L.B. Alemany, W. Lu, J.M. Tour, Improved synthesis of graphene oxide, Acsnano 4 (2010), 8 4806–4814.
[47] R.B. Rakhi, H.N. Alshareef, Enhancement of the energy storage properties of supercapacitors using graphene nanosheets dispersed with metal oxide-loaded carbon nanotubes, J. Power Sources 196 (2011) 8858–8865.
[48] C. Mahendirana, T. Maiyalaganb, K. Scottb, A. Gedanken, Synthesis of a carbon-coated NiO/MgO core/shell nanocomposite as a Pd electro-catalyst support for ethanol oxidation, Mater. Chem. Phys. 128 (2011) 341–347.
[49] (a) L.T.M. Nguyen, H. Park, M. Banu, J.Y. Kim, D.H. Youn, G. Magesh, W.Y. Kim, J.S. Lee, Catalytic CO2 Hydrogenation to formic acid over carbon nanotube-graphene supported PdNi, RSC Adv. 00 (2013) 1–3;
(b) M.K. Kumar, Niki S. Jha, S. Mohan, S.K. Jha, Reduced graphene oxide-supported nickel oxide catalyst with improved CO tolerance for formic acid electrooxidation, Int. J. Hydrogen Energy 39 (125) (2014) 2–12577.
[50] S. Pichaikaran, P. Arumugam, Vapor phase hydrodeoxygenation of anisole over ruthenium and nickel supported mesoporous aluminosilicate, Green Chem. (2016), https://doi.org/10.1039/C5GC01854D.
[51] Z. Zanga, X. Zenga, M. Wanga, W. Hua, C. Liub, X. Tanga, Tunable photoluminescence of water-soluble AgInZnS–grapheneoxide (GO) nanocomposites and their application in-vivo bioimaging, Sens. Actuat. B 252 (2017) 1179–1186.
[52] P.K. Aneesh, S.R. Nambiar, T.P. Rao, A. Ajayaghosh, Electrochemically synthesized partially reduced graphene oxide modified glassy carbon Electrode for individual and simultaneous voltammetric determination of ascorbic acid, dopamine and uric acid, Anal. Methods (2014), https://doi.org/10.1039/C4AY00043A.
[53] J. Wei, Z. Zang, Y. Zhang, M. Wang, J. Du, X. Tang, Enhanced performance of light-controlled conductive switching in hybrid cuprous oxide/reduced graphene oxide (Cu2O/rGO) nanocomposites, Optical Lett. 5 (2017) 42.
[54] M. Hsin Yeh, L. Yin Lin, C. Liang Sun, Y. An Leu, J. Ting Tsai, C. Yu Yeh, R. Vittal, K. Chuan Ho, Multiwalled carbon nanotube@reduced graphene oxide nanoribbon as the counter electrode for dye-sensitized solar cells, J. Phys. Chem. C 118 (2014) 16626–16634.
[55] Y. Feng, D. Bin, B. Yan, Y. Du, T. Majima, W. Zhou, Porous bimetallic PdNi catalyst with high electrocatalytic activity for ethanol electrooxidation, J. Colloid Interface Sci. 493 (2017) 190–197.
[56] Yanchun Zhao, Xiulin Yang, Jianniao Tian, Fengyang Wang, Lu Zhan, Methanol electro-oxidation on Ni@Pd core-shell nanoparticles supported on multi-walled carbon nanotubes in alkaline media, Int. J. Hydrogen Energy 35 (2010) 3249–3257.
[57] V. Gunasekaran, P. Arumugam, Up-gradation of α-tetralone to jet-fuel range hydrocarbons by vapour phase hydrodeoxygenation over Pd-Ni/SBA-16 catalysts, J. Energy (2017) 09–038.
[58] T. Maiyalagan, K. Scott, Performance of carbon nanofiber supported Pd–Ni catalysts for electro-oxidation of ethanol in alkaline medium, J. Power Sources 195 (2010) 5246–5251.
[59] R. Pattabiraman, Appl. Catal. A 153 (1997) 9.
[60] R.N. Singh, A. Singh and Anindita, Electrocatalytic activity of binary and ternary composite films of Pd, MWCNT and Ni, Part II: Methanolelectrooxidation in 1 M KOH, i, Int. J. Hydrogen Energy 3 (4) (2009) 2052–2057.
[61] Y. Zhao, L. Zhan, J. Tian, S. Nie, Z. Ning, Enhancedelectrocatalytic oxidation of methanol on Pd/ polypyrroleegrapheme in alkaline medium, Electrochim. Acta 56 (2011) 1967–1972.
[62] Z. Zhang, L. Xin, K. Sun, W. Li, Pd-Ni electrocatalysts for efficient ethanol oxidation reaction in alkaline electrolyte, Int. J. Hydrogen Energy 36 (2011) 12686–12697.
[63] N. Li, Y. Xian Zeng, S. Chen, C. Wei Xu, Pei-Kang Shen, Ethanol oxidation on Pd/C enhanced by MgO in alkaline medium, Int. J. Hydrogen Energy 39 (2014) 16015–16019.
[64] E. AngwenyiMonyoncho, S. Ntais, N. Brazeau, J. JhouWu, C. LiangSun, E.A. Baranova, Role of the metal-oxide support in the catalytic activity of Pd nanoparticles for ethanol electrooxidation in alkaline media, ChemElectroChem 3 (2016) 218–227.